

# Nucleo-cytosolic Shuttling of FoxO1 Directly Regulates Mouse *Ins2* but Not *Ins1* Gene Expression in Pancreatic Beta Cells (MIN6)<sup>\*[5]</sup>

Received for publication, November 18, 2010, and in revised form, February 14, 2011. Published, JBC Papers in Press, February 18, 2011, DOI 10.1074/jbc.M110.204248

Gargi Meur<sup>‡1</sup>, Qingwen Qian<sup>‡1</sup>, Gabriela da Silva Xavier<sup>‡</sup>, Timothy J. Pullen<sup>‡</sup>, Takashi Tsuboi<sup>§</sup>, Caroline McKinnon<sup>‡¶</sup>, Laura Fletcher<sup>¶</sup>, Jeremy M. Tavaré<sup>¶</sup>, Stephen Hughes<sup>||</sup>, Paul Johnson<sup>||</sup>, and Guy A. Rutter<sup>‡2</sup>

From the <sup>‡</sup>Section of Cell Biology, Division of Diabetes, Endocrinology and Metabolism, Department of Medicine, Faculty of Medicine, Imperial College London, London SW7 2AZ, United Kingdom, the <sup>¶</sup>Henry Wellcome Laboratories for Integrated Cell Signalling and Department of Biochemistry, School of Medical Sciences, University Walk, University of Bristol, Bristol BS8 1TD, United Kingdom, the <sup>||</sup>Nuffield Department of Surgery, John Radcliffe Hospital, Oxford OX3 9DU, United Kingdom, and the <sup>§</sup>Department of Life Sciences, University of Tokyo, Tokyo 153-8902, Japan

The Forkhead box transcription factor FoxO1 regulates metabolic gene expression in mammals. FoxO1 activity is tightly controlled by phosphatidylinositol 3-kinase (PI3K) signaling, resulting in its phosphorylation and nuclear exclusion. We sought here to determine the mechanisms involved in glucose and insulin-stimulated nuclear shuttling of FoxO1 in pancreatic  $\beta$  cells and its consequences for *preproinsulin* (*Ins1*, *Ins2*) gene expression. Nuclear-localized endogenous FoxO1 translocated to the cytosol in response to elevated glucose (3 versus 16.7 mM) in human islet  $\beta$  cells. Real-time confocal imaging of nucleo-cytosolic shuttling of a FoxO1-EGFP chimera in primary mouse and clonal MIN6  $\beta$  cells revealed a time-dependent glucose-responsive nuclear export, also mimicked by exogenous insulin, and blocked by suppressing insulin secretion. Constitutively active PI3K or protein kinase B/Akt exerted similar effects, while inhibitors of PI3K, but not of glycogen synthase kinase-3 or p70 S6 kinase, blocked nuclear export. FoxO1 overexpression reversed the activation by glucose of pancreatic duodenum homeobox-1 (*Pdx1*) transcription. Silencing of FoxO1 significantly elevated the expression of mouse *Ins2*, but not *Ins1*, mRNA at 3 mM glucose. Putative FoxO1 binding sites were identified in the distal promoter of rodent *Ins2* genes and direct binding of FoxO1 to the *Ins2* promoter was demonstrated by chromatin immunoprecipitation. A 915-bp glucose-responsive *Ins2* promoter was inhibited by constitutively active FoxO1, an effect unaltered by simultaneous overexpression of PDX1. We conclude that nuclear import of FoxO1 contributes to the suppression of *Pdx1* and *Ins2* gene expression at low glucose, the latter via a previously unsuspected and direct physical interaction with the *Ins2* promoter.

The mechanisms through which changes in glucose concentration regulate the expression of the *preproinsulin* and other genes in pancreatic islet  $\beta$  cells are only partly understood (1, 2). Enhanced secretion of insulin, and the rebinding of the released hormone to pancreatic  $\beta$ -cell insulin receptors, may play an important role in mediating some of the effects of nutrients in this cell type (3–8). Indeed, Bouche *et al.* (9) recently demonstrated that insulin improves glucose-stimulated insulin secretion in healthy humans. However, the identity of the downstream transcription factors, and/or repressors, which mediate the effects of insulin and glucose, is still incompletely defined.

Forkhead transcription factors, characterized by the presence of a 100-amino acid winged helix domain, are implicated in the control of a variety of cellular processes (10). FoxO1 (previously termed FKHR), is a member of the Forkhead box (FOX)<sup>3</sup> subclass whose deletion results in early embryonic lethality in mice (11). Activation by insulin of type 1 phosphoinositide 3-phosphokinases (PI3Ks) and protein kinase B (PKB/Akt) (12) results in the phosphorylation of FoxO1 at Ser<sup>256</sup> (supplemental Fig. S1, A and B) and causes the translocation of FoxO1 from the nucleus to the cytoplasm (13, 14). This is followed by enhanced degradation of FoxO1 (15) and thereby depression (16) of target genes. Conversely, in pancreatic  $\alpha$  cells, nuclear accumulation of FoxO1 when glucose and insulin concentrations are low leads to the activation of the preproglucagon gene (17).

Suggesting an important role as a repressor of pancreatic islet  $\beta$ -cell gene expression, inactivation of a single allele of the *FoxO1* gene in mice rescued the deleterious effect of deleting insulin receptor substrate-2 (11, 18). Conversely, transgenic overexpression of FoxO1 in the liver and in  $\beta$  cells of mice led to abnormal glucose tolerance *in vivo* and defective glucose-stimulated insulin secretion (19). Finally, overexpression of FoxO1 in clonal  $\beta$ TC-3 cells reversed the activation by Foxa2 (HNF3 $\beta$ ) of a fragment of the proximal promoter of pancreatic duodenal

\* This work was supported by Juvenile Diabetes Research Fund (JDRF) Project Grant 1-2003-235, Wellcome Trust Programme Grants 067081/Z/02/Z and 081958/Z/07/Z, and Research Leave Fellowship (to G. A. R.) as well as grants from the BBSRC and MRC (UK), and the European Union (FP6, Save Beta).

[5] The on-line version of this article (available at <http://www.jbc.org>) contains supplemental Figs. S1–S3 and Table S1.

⌘ Author's Choice—Final version full access.

<sup>1</sup> Both authors contributed equally to this work.

<sup>2</sup> To whom correspondence should be addressed: Section of Cell Biology, Faculty of Medicine, Imperial College London, Sir Alexander Fleming Bldg., Exhibition Rd., London SW7 2AZ, UK. Tel.: 44-20-759-43340; Fax: 44-20-579-43351; E-mail: [g.rutter@imperial.ac.uk](mailto:g.rutter@imperial.ac.uk).

<sup>3</sup> The abbreviations used are: FOX, Forkhead box; DBE, Daf-16 binding element; GSK3, glycogen synthase kinase-3; IRE, insulin response element; MafA, v-maf musculoaponeurotic fibrosarcoma oncogene homolog A; NeuroD, neurogenic differentiation 1; PI3K, phosphatidylinositol 3-kinase; PKB, protein kinase B/Akt.

## FoxO1 Regulation of $\beta$ Cell Genes

homeobox 1 (*Pdx1*) (20), a key regulator of  $\beta$  cell differentiation (2).

Another study has demonstrated that FoxO1 translocated from the nucleus to the cytosol of MIN6  $\beta$  cells in response to elevated glucose concentrations in a mechanism involving enhanced insulin secretion and signaling through PI3K (21). However, neither the kinetics, nor the molecular basis of the nuclear-cytosolic shuttling of FoxO1 was explored in detail in the latter study. Moreover, although a possible role for FoxO1 in the regulation of the *Chop* promoter was identified (21), the role in the regulation of *Pdx1* and *preproinsulin* transcription was not explored (21).

By imaging the dynamics of FoxO1-EGFP cytoplasmic-nuclear shuttling, and the activity of potential target genes, in single primary human and mouse  $\beta$  cells and in clonal MIN6 cells, we show here that: (a) FoxO1 translocation occurs rapidly (within 10–20 min) after exposure to high glucose or insulin; (b) involves the activation of PI 3-kinase and PKB/Akt, but not ribosomal protein 70 kDa S6 kinase (p70 S6K) or glycogen synthase kinase-3, (c) blocks *Pdx1* and *Ins2* transcription by separate and at least partly independent mechanisms, including the direct binding of FoxO1 to the preproinsulin promoter.

### EXPERIMENTAL PROCEDURES

**Reagents**—Dulbecco's modified Eagle's medium (DMEM) was obtained from Sigma. Lipofectamine 2000<sup>TM</sup> and Lipofectamine RNAi Max<sup>TM</sup>, Trizol were from Invitrogen (Carlsbad, CA), dual-luciferase assay kit was from Promega (Southampton, UK) and LY294002, SB216763, and SB415286 were from Calbiochem (Nottingham, UK).

**Plasmids, pFoxO1-EGFP**—Human FKHR was cloned by PCR as described elsewhere (17). The full-length FKHR/FoxO1 clone was then amplified by PCR to add Xho1 and Sal1 sites and cloned into pCINeo downstream of EGFP. The FoxO1-EGFP fragment was further subcloned into pShuttle and recombined in adenoviral vector pAdeasy as described (22). cDNA encoding a constitutively active (CA) FoxO1 was generated by substitution of Ser<sup>256</sup> to Ala by site directed mutagenesis (Agilent Technologies Inc, Cheshire, UK) in the FoxO1-EGFP-pShuttle vector, which was then used to generate the adenoviral vectors.

Plasmids based on vector pCMV5 (Invitrogen) and bearing constitutively active (-DD; containing substitutions of Thr<sup>308</sup> and Ser<sup>473</sup> for Asp) and membrane-targeted forms of PKB, (*myr*PKB) were kindly provided by Professor B. Hemmings (Friedrich Miescher Institute, Basel). Plasmid pCMV-RL carrying *Renilla reniformis* cDNA under cytomegalovirus promoter control and pGL3 Basic (23) were from Promega. Generation of pCMV.Pdx1, the full-length human *Pdx1* cDNA bearing a *c-myc* epitope tag (24) and plasmids bearing the active catalytic subunit of PI3K, modified with the addition of a CAAX box, or a dominant-negative form of the regulatory subunit lacking the p100-binding domain ( $\Delta$ p85) (25) are described elsewhere (24).

**pIns2.Luc<sub>FF</sub>**—Total DNA was extracted from MIN6 cells and the *Ins2* promoter was PCR amplified using primers R1 fwd and R2 rev as described later in this section ("Chromatin Immunoprecipitation"). The fragment was cloned upstream of a cDNA encoding humanized firefly luciferase in plasmid pGL3 (Promega). The resulting *pIns2.Luc<sub>FF</sub>* plasmid consisted of a 915 bp

fragment of the mouse *Ins2* promoter spanning nucleotides -907 to +8 bp with respect to the transcriptional start site. The deletion mutant (*Ins2* $\Delta$ <sup>Region1</sup>) was generated by removing the first 290 bp from *pIns2.Luc<sub>FF</sub>* using an internal Sac1 site. The Herpes simplex virus thymidine kinase (TK) promoter was excised from pRL-TK (Promega) and inserted into pGL3 Basic to create pGL3-TK in which expression of firefly luciferase is driven by the TK promoter. The 290 bp region 1 of mouse *Ins2* promoter was inserted upstream of the TK promoter between KpnI and SacI sites.

**MIN6 Cell Culture**—Clonal MIN6  $\beta$ -cells (26) were used between passages 20 and 30 and grown in DMEM supplemented with 15% (v/v) heat-inactivated fetal calf serum (Invitrogen), 25 mM glucose, 2 mM glutamine, 50  $\mu$ M  $\beta$ -mercaptoethanol, 100 IU/ml penicillin, and 100  $\mu$ g/ml streptomycin. Cells were cultured in a humidified atmosphere at 37 °C with 5% CO<sub>2</sub>, as previously described (23).

**Human and Mouse Islet Isolation**—Islets were isolated from cadaveric donors according to standard procedures (27) following local ethical procedures (Charing Cross Ethics Committee REC 07/H0711/114). Mouse islets were prepared as described elsewhere (28). The islets were allowed to recover for a week in culture medium (RPMI supplemented with 10% FCS, 2 mM glutamine, and 11 mM glucose).

**Transfection and Transduction**—MIN6 cells seeded onto poly-L-lysine-coated coverslips were transfected with pFoxO1-EGFP (1  $\mu$ g/ml) alone or with other plasmids (each at 1  $\mu$ g/ml) using Lipofectamine 2000<sup>TM</sup>, according to the manufacturer's instructions. Islets were partially dissociated by incubation in Hank's-based cell dissociation buffer (Invitrogen) for 10 min and by vigorous pipetting. Islet clusters were seeded on poly-L-lysine coated coverslips for a day and transduced with FoxO1-EGFP adenoviral particles of a multiplicity of infection (MOI) of 20–25 for 6 h and subsequently allowed to express the protein for 24–48 h in fresh culture media.

**Dual Luciferase Assay**—MIN6 cells seeded on 12-well plates at 70% confluency were transfected with a mixture of 450 ng pIns2<sub>FF</sub> and 1 ng of pCMV<sub>Ren</sub> or 500 ng of TK<sub>FF</sub> and 100 ng of TK<sub>Ren</sub> using Lipofectamine 2000. After 4 h, media was replaced and adenoviral particles were added at 20–30 MOI where indicated. Cells were incubated for a further 16 h and then media changed to allow culture for 16–20 h at 3, 25, or 30 mM glucose. Luciferase assay was carried out using a Dual-Luciferase kit (Promega) and a Lumat LB 9507 Luminometer following manufacturer's instructions.

**Confocal Imaging and Image Analysis**—After culturing in DMEM-based medium at the required concentrations of glucose and insulin, MIN6 cells were transferred into Krebs-Ringer bicarbonate (KRB) buffer (125 mM NaCl, 3.5 mM KCl, 1.5 mM CaCl<sub>2</sub>, 0.5 mM MgSO<sub>4</sub>, 0.5 mM KH<sub>2</sub>PO<sub>4</sub>, 25 mM NaHCO<sub>3</sub>, and 10 mM Na<sup>+</sup>-Hepes, equilibrated with 95:5 O<sub>2</sub>/CO<sub>2</sub>). Confocal microscopy was performed with a Leica TCS DM IRBE inverted confocal microscope (488 nm excitation;  $\times$ 63 oil immersion objective) controlled with TCS-NT4 software (Leica). The extent of FoxO1-EGFP translocation to the nucleus was quantified in regions of interest (ROI) as follows. Fluorescence intensity within selected cytosolic or

nuclear regions was measured using on-board TCS-NT software, and the mean ratio of cytosol:nuclear intensity obtained.

**siRNA Transfection and Real-time qRT-PCR Analysis**—MIN6 cells seeded on 6-well plates were transfected with 20 nM of either scrambled (prepared using a template, 5'-AAATGTC-CCCCTCAGCGTGTCTGTCTG-3' and a Silencer siRNA construction kit, Ambion, Huntingdon, UK) or SiGENOME SMARTpool™ siRNA (Dharmacon, Thermo Fisher Scientific, Lafayette, CO) using Lipofectamine RNAiMax™ for 48 h in culture media before subsequent culture in media containing 3 or 30 mM glucose. Total RNA was prepared with Trizol and treated with DNase 1 (Ambion). RNA (2  $\mu$ g) was reverse-transcribed using High Capacity cDNA Reverse Transcription kit. Real-time PCR was carried out with cDNA (equivalent of 20 ng input RNA) using Power SYBR Green master mix (ABI Biosystems) in a 7500 Fast Real-Time PCR system (ABI Biosystems) and analyzed by comparative  $C_t$  method. All real-time primers (supplemental Table S1) were generated using ABI Primer Express 3.0 except for FoxO1 the SF QuantiTect™ (Qiagen) primers were used and were predicted to produce a single unique product under the high stringency conditions deployed.

**Western Blotting**—Protein analysis was carried out as described elsewhere (29). The antibodies used were rabbit monoclonal anti-FoxO1 (1:1000, C29H4 Cell Signaling Technology, Danvers, MA), anti-Phospho-FoxO1 Ser-256 (1:1000, Cell Signaling Technology), monoclonal anti- $\alpha$  tubulin (1:10,000, Sigma clone B-5-1-2) and HRP-linked secondary antibodies (1:10000, GE Healthcare).

**Chromatin Immunoprecipitation**—ChIP was performed as described elsewhere (30). Briefly, MIN6 cells were cultured in medium containing 3 mM glucose for 16 h before stimulation with 3 or 30 mM glucose for 20 h, and then cross-linking with 1% formaldehyde and sonication to obtain fragments of chromatin of  $\sim$ 0.5 kb. DNA-protein complexes were immunoprecipitated with a rabbit monoclonal antibody against FoxO1 (C29H4, Cell Signaling Technology, Danvers, MA) or ChIP-grade immunoglobulin G (Sigma), and protein-G-agarose/salmon sperm DNA (Millipore), followed by digestion with proteinase K (Roche Applied Science). The resulting DNA was extracted using phenol-chloroform and precipitated with ethanol. Regions of interest were PCR amplified using Accuprime™ TaqDNA polymerase (Invitrogen) and primers (R1 fwd: tctcccaggtaccagagt, R1 rev: agccagctgtctccatctgt, R2 fwd: aactggttcatcaggccatc, R2 rev: ttagggctggtggttactgg, R3 fwd: ccagtaaccaccagccctaa, R3 rev: caaaggtgctgcttgacaaa) specific to regions ( $\sim$ 200 bp) encompassing the putative FoxO1 binding sites.

**Immunostaining and Confocal Imaging**—MIN6 cells grown on glass coverslips and transduced with adenoviral vectors as indicated. Immunostaining was carried out using the following antibodies; monoclonal anti-Myc antibody (1:200; Roche), polyclonal anti-Swine insulin (1:200; DakoCytomation, Ely, UK), anti-FoxO1 (1:200) and Alexa 488- or 564-coupled secondary antibodies (1:500; Molecular Probes) and confocal imaging was carried out as described elsewhere (29).

**Statistical Analysis**—Data analyzed using one-tailed Student's *t* test for paired data with Microsoft Excel™, or two-

tailed Student's *t* test and two-way ANOVA with Bonferroni correction using GraphPad Prism™ where appropriate.

## RESULTS

**Elevated Glucose Concentrations or Insulin Cause Translocation of FoxO1-EGFP from the Nucleus to the Cytosol**—Beta cell clusters derived from partially-dissociated human islets showed, upon incubation at 3 or 16.7 mM glucose for 16 h and subsequent staining with anti-FoxO1 or insulin antibodies, differential staining of endogenous FoxO1 in the nucleus and cytosol (Fig. 1, A and B), indicating that FoxO1 translocates from the nucleus in response to the sugar. To analyze the kinetics and molecular mechanisms involved in FoxO1 nuclear exclusion more closely, we monitored the subcellular localization of FoxO1-EGFP in primary mouse  $\beta$  cells incubated at 16.7 mM glucose for different time periods up to 1 h (Fig. 1, C and D). Cells were again fixed with formaldehyde and immunostained with an anti-insulin antibody. While FoxO1 was predominantly localized in the nucleus after overnight incubation in 3 mM glucose, exposure to the elevated sugar concentration triggered significant cytosolic translocation after 45–60 min of stimulation. Real-time imaging of FoxO1-EGFP dynamics in single living  $\beta$  cells derived from mouse islets (Fig. 2, A–D) or MIN6  $\beta$  cell lines (Fig. 2, E–H) showed that whereas the initial, predominantly nuclear localization of FoxO1 was maintained during incubation in 3 mM glucose, addition of 16.7 (Fig. 2, A and B) or 30 mM glucose (Fig. 2, E and F), or 20 (Fig. 2C) or 200 nM (Fig. 2, C, G, H) insulin caused a progressive increase in cytosolic fluorescence at the expense of nuclear fluorescence. These changes were clearly detectable after 10–20 min of exposure to either stimulus. However, quantitation of fluorescence changes during the time course revealed that while insulin caused a near 4-fold increase in cytosolic to nuclear fluorescence after 60 min, the response to 30 mM glucose was more modest with a maximum increase of twice the initial value. While we were unable in this case to confirm that the examined cell was a  $\beta$  cell, from our staining for insulin in these cultures (above), and a vast quantity of existing literature in the rodent (e.g. Ref. 31),  $\beta$  cells are likely to comprise 70–75% of the cells in these cultures. Here again, in individual cells, we observed closely similar data to that obtained from the “cross-sectional” studies obtained from collections of  $\beta$  cells (Fig. 1C) in terms of the initial and final cytosol:nucleus staining and the time course of the changes in this parameter.

Next, we determined whether the stimulatory effect of high glucose was due to the secreted insulin acting through an auto-crine loop (8). MIN6 cells were maintained for 6 h in serum-containing medium at either low (0.5 mM) or high (25 mM) glucose in the additional presence of 20 nM insulin or 200  $\mu$ M diazoxide (Fig. 3, A and B). By opening the ATP-sensitive  $K^+$  channels, diazoxide causes hyperpolarization of the plasma membrane and thereby an essentially complete inhibition of glucose-stimulated insulin secretion of the MIN6 cells (32). Added insulin efficiently mimicked the effects of 25 mM glucose. The effects of glucose, but not those of insulin, were completely suppressed by diazoxide (Fig. 3, A and B).

## FoxO1 Regulation of $\beta$ Cell Genes

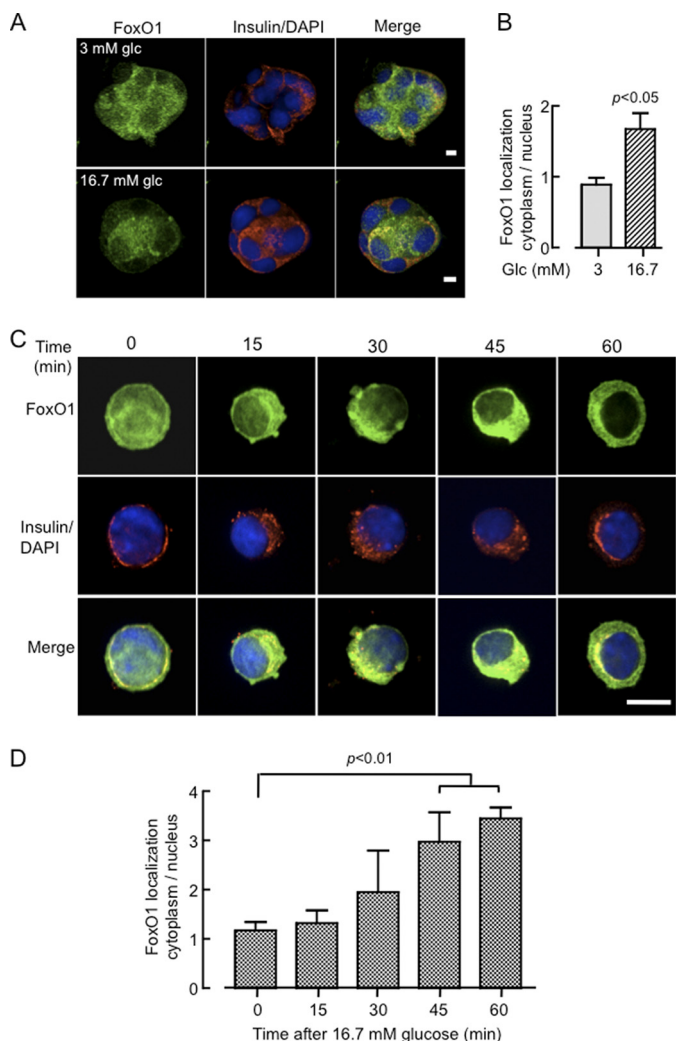


**FIGURE 1. Imaging the effects of glucose and insulin on the subcellular localization of endogenous FoxO1 or overexpressed FoxO1-EGFP in primary human and mouse  $\beta$ -cells.** *A*, partially dissociated human islets seeded on coverslips for 1 day in 11 mM glucose were subsequently incubated for 16 h in 3 or 16.7 mM glucose, were formaldehyde-fixed, permeabilized, and immunostained with anti-FoxO1 and anti-insulin antibodies, and subsequently with Alexa Fluor-488- and -564-coupled secondary antibodies, while DAPI was used for nuclear staining. Cell clusters containing insulin-positive cells were imaged by confocal microscopy taking Z cross-sections at 0.2  $\mu$ m spacing along the entire depth of the clusters. The three-dimensional "opacity" (Volocity™ software) view is presented. Scale bar, 10  $\mu$ m. *B*, ratio of fluorescence quantified within regions of interest selected in the cytosol and nucleus in the central cross-sections of single islet  $\beta$  cells and calculated from 25–30 individual cells. The bar shows mean  $\pm$  S.E. analyzed by two-tailed *t* test. *C*, dissociated mouse islet cells plated on coverslips were transduced with FoxO1-EGFP-expressing adenovirus (20–25 MOI) and incubated for 36 h to allow expression. Following overnight incubation in 3 mM glucose, cells were exposed to either 3 or 16.7 mM glucose for the indicated time before fixation and immunostaining with anti-insulin antibody as described in *A*. Images show typical distribution of FoxO1-EGFP from 20–30 cells studied per condition from three independent experiments. Scale bar, 10  $\mu$ m. *D*, ratio of fluorescence quantified from *C*, as described in *B*. Bar shows mean  $\pm$  S.E. analyzed by two-tailed *t* test all compared to 0 time point.

*The Effects of Glucose and Insulin on FoxO1-EGFP Translocation Are Due to Activation of PI 3-Kinase Signaling*—We sought next to study if the effects of glucose were mediated by released insulin, as opposed to the action of co-secreted factors (ATP, Zn<sup>2+</sup> etc) in which case the action of glucose should be inhibited by the blockade of signaling downstream of the insulin receptor. To test this possibility, we inhibited PI3K activity

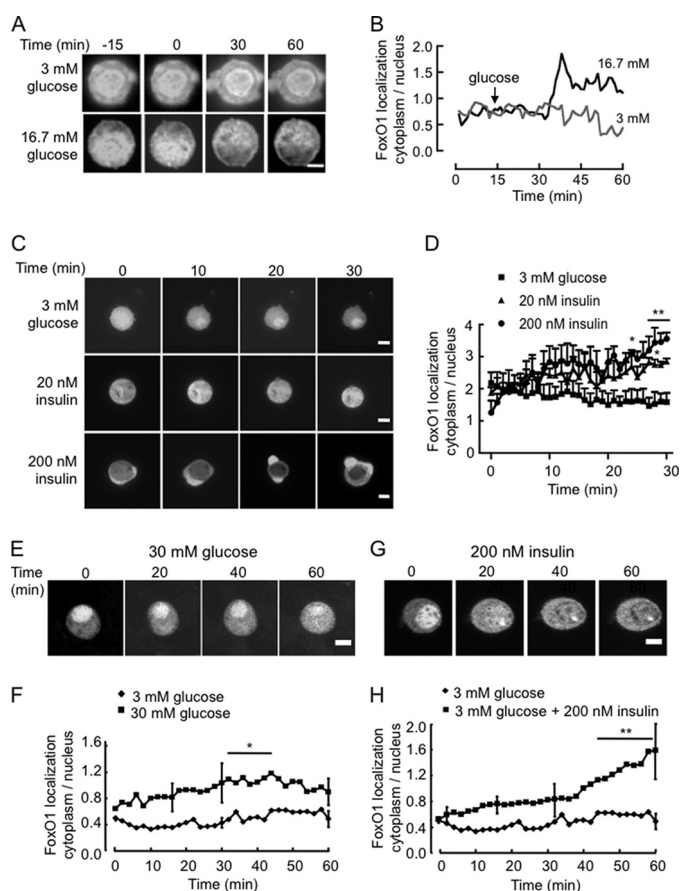


**FIGURE 2. Real-time dynamic imaging of the effects of glucose and insulin on the subcellular localization of FoxO1-EGFP.** Single primary  $\beta$  cells derived from mouse islets (*A* and *C*) or clonal MIN6 cells (*E* and *G*) were infected with FoxO1-EGFP-expressing adenovirus and cultured for 48 h in complete medium and then overnight in 3 mM glucose. Cells were then transferred to the heated stage of a Leica SP2 confocal microscope in KRBB containing 3 mM glucose. Images were captured every 2 min up to 60 min, either 15 min (*A*) or immediately before and then after the addition of 16.7 mM (*A*) or 30 mM (*E*) glucose, 20 nM (*C*) or 200 nM insulin in (*C*, *G*) as indicated. *Traces* in *B* are typical of the single cells seen in *A* and are presented to distinguish the glucose-dependent effects above basal fluctuations. All other traces (*D*, *F*, *H*) show the mean  $\pm$  S.E. from  $\geq 3$  independent experiments. Error bars are included only for the 15, 30, and 60 min time points for clarity. \*, *p* < 0.05. Scale bar, 10  $\mu$ m (5  $\mu$ m for *A*).

with either the pharmacological agent LY294002 or by expression of a dominant-negative form of the PI3K adaptor subunit  $\Delta$ p85 (25). The latter was expected to prevent the recruitment of the catalytic (p110) subunit of PI3K to the phosphorylated adaptor molecules (IRS1, IRS2, Shc, etc.) (24). Incubation with LY294002 or the expression of  $\Delta$ p85 led to a complete suppression of the effects of glucose and insulin on the subcellular localization of FoxO1 (Fig. 4, *A* and *B*). Conversely, expression of a constitutively active, membrane-associated form of p110 (p100.CAAX) led to the translocation of FoxO1 from the nucleus at low (0.5 mM) as well as elevated (25 mM) glucose concentrations.

To explore the signaling pathways acting downstream of PI3K, we determined whether FoxO1 translocation to the cytosol could be induced by a constitutively active form of PKB/Akt, PKB-DD (Thr<sup>308</sup> and Ser<sup>473</sup> substituted with Asp), or by a membrane-targeted constitutively active version of PKB (PKB-*myr*). Cotransfection with either construct resulted in a signif-

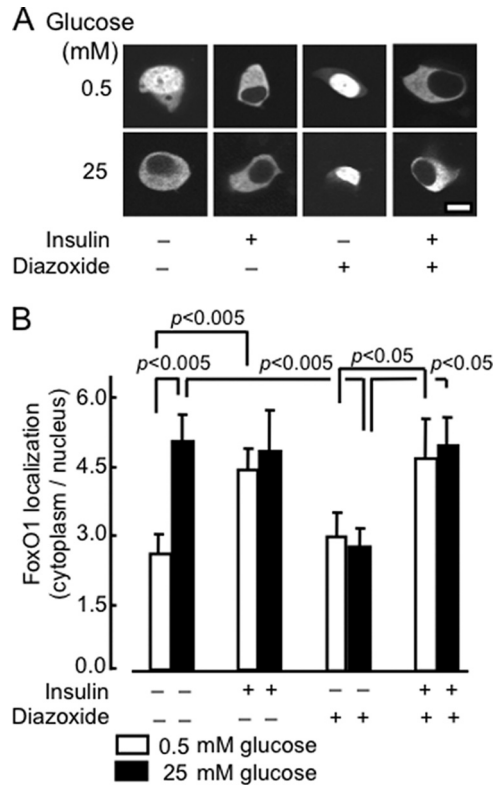


**FIGURE 3. Role of secreted insulin on the effects of glucose on FoxO1-EGFP translocation.** *A*, after 24 h of transient transfection with pFoxO1-EGFP, MIN6 cells were incubated at varying concentrations of insulin (0, 20 nM), glucose (0.5, 25 mM), or DAO (diazoxide, 20 and 200  $\mu$ M) for 1 h in medium prior to imaging. *B*, distribution of FoxO1 between the cytosol and nucleus. Data show ratio (mean  $\pm$  S.E.,  $n = 20$ –50 cells from three separate experiments).

inant increase in the ratio of cytosolic to nuclear FoxO1 at low glucose concentrations (Fig. 4, *C* and *D*), consistent with a role for active PKB. Ribosomal S6 kinase (p70 S6 K) (33) and glycogen synthase kinase (34) have both recently been shown to be activated by glucose and insulin, as well as other growth factors in clonal rat  $\beta$  cells (INS-1). However, we observed here that pre-incubation of MIN6 cells with the p70 S6 kinase inhibitor rapamycin had no effect on the translocation of FoxO1 provoked by either 25 mM glucose or 20 nM insulin. Similarly, treatment with either of two structurally distinct GSK3 inhibitors, SB216763 or SB415286 (35) had no effect on the subcellular distribution of FoxO1 at either low or high glucose concentrations (Fig. 4, *C* and *D*) arguing that neither of the downstream kinases is involved in stimulating the nuclear export of FoxO1.

*Modulation of FoxO1 Expression Affects Mouse Ins2 mRNA Levels; Evidence for a Direct Interaction of FoxO1 with the Promoter of the Corresponding Gene*—Given that FoxO1 is a key transcription factor in metabolic gene regulation in response to glucose and insulin, we next examined the effects of FoxO1 silencing on some of the most important genes involved in  $\beta$ -cell glucose metabolism. A reduction (>70%) in FoxO1 expression (Fig. 5, *A* and *B*) in MIN6 cells, achieved by transfection of FoxO1 siRNA for 48 h led, upon subsequent culture in 3 or 30 mM glucose for another 12–16 h, to a significant rise in basal *Ins2* mRNA levels at 3 mM glucose

(Fig. 5*B*), but not in *Ins1*, *Pdx1* (Fig. 5*B*) or *MafA* and *NeuroD* (supplemental Fig. S2) mRNA levels. Despite displaying an elevated basal *Ins2* mRNA level, FoxO1-silenced cells appeared to retain the glucose inducibility of *Ins2* expression. Thus, basal and glucose-induced expression levels were significantly different, though the fold rise in response to high glucose was less when compared with control cells (scrambled siRNA). Furthermore, the level of *Ins2* mRNA after treatment with 30 mM glucose did not differ significantly in cells silenced or not for FoxO1. A tendency toward an increased basal level of expression, though not reaching significance, was also observed for *Pdx1*, but not for *Ins1*, *MafA* or *NeuroD* mRNAs (supplemental Fig. S2). On the other hand, overexpression of a dephosphomimetic (Ser<sup>256</sup>>Ala), constitutively-active and nuclearly localized form of FoxO1 (FoxO1-CA) led to a remarkable inhibition of both *Ins2* and *Pdx1*, but not *Ins1*, mRNA expression (Fig. 5*C*). Because of its constitutive presence in the nucleus, FoxO1-CA thus overcomes the effect of high glucose and thereby helps to identify possible repressive effects of this factor on genes while over-riding its intrinsic regulation. It should be emphasized that the real-time PCR primers designed against each of the genes studied, including *Ins1* and *Ins2*, recognized exclusive regions within the transcribed template, with minimal overlap between genes. Thus, each pair of primers amplified a single and specific product under the high stringency PCR conditions deployed (see “Experimental Procedures” for further details). The differential regulation of the two rodent insulin genes by FoxO1 would appear therefore to be a *bona fide* phenomenon whose mechanisms were studied further below.

Importantly, the above findings are consistent with the negative regulatory role of FoxO1 toward insulin/IGF-induced  $\beta$ -cell growth and proliferation (11) and inhibition of *Pdx1* action at the insulin promoter by competition with the stimulatory factor FoxA2/HNF3 $\beta$  for the same binding site (20, 36). The above findings also raise the possibility of a direct inhibition of mouse *Ins2*, but not *Ins1* expression by FoxO1. Indeed, a search for consensus FoxO1 binding sites, namely the insulin response element (IRE) and the Daf-16 binding element (DBE) in the rodent *Ins2* promoter region extending up to 2-kb upstream from the transcription start site revealed three regions of partial identity (Fig. 6*A*), which were absent in the *Ins1* promoter. Region 1 in the distal *Ins2* promoter contained two such binding sites starting at -768 and -673 bp upstream of transcription start site, while region 2 was identified in the proximal promoter (-141). To determine if these elements were genuine FoxO1 binding sites with physiological relevance, a chromatin immunoprecipitation experiment was carried out using cross-linked DNA from MIN6 cells cultured in 3 or 30 mM glucose and a rabbit monoclonal anti-FoxO1 antibody. As shown in Fig. 6*B*, and quantified in Fig. 6*C*, cells maintained overnight at 3 mM glucose displayed significant FoxO1 binding to the promoter region 1, to a smaller, but nevertheless significant extent to region 2, but not to region 3. Conversely, incubation of cells at 30 mM glucose effectively eliminated binding of FoxO1 to these regions. The chromatin immunoprecipitation experiments with FoxO1 antibody were validated by PCR

## FoxO1 Regulation of $\beta$ Cell Genes

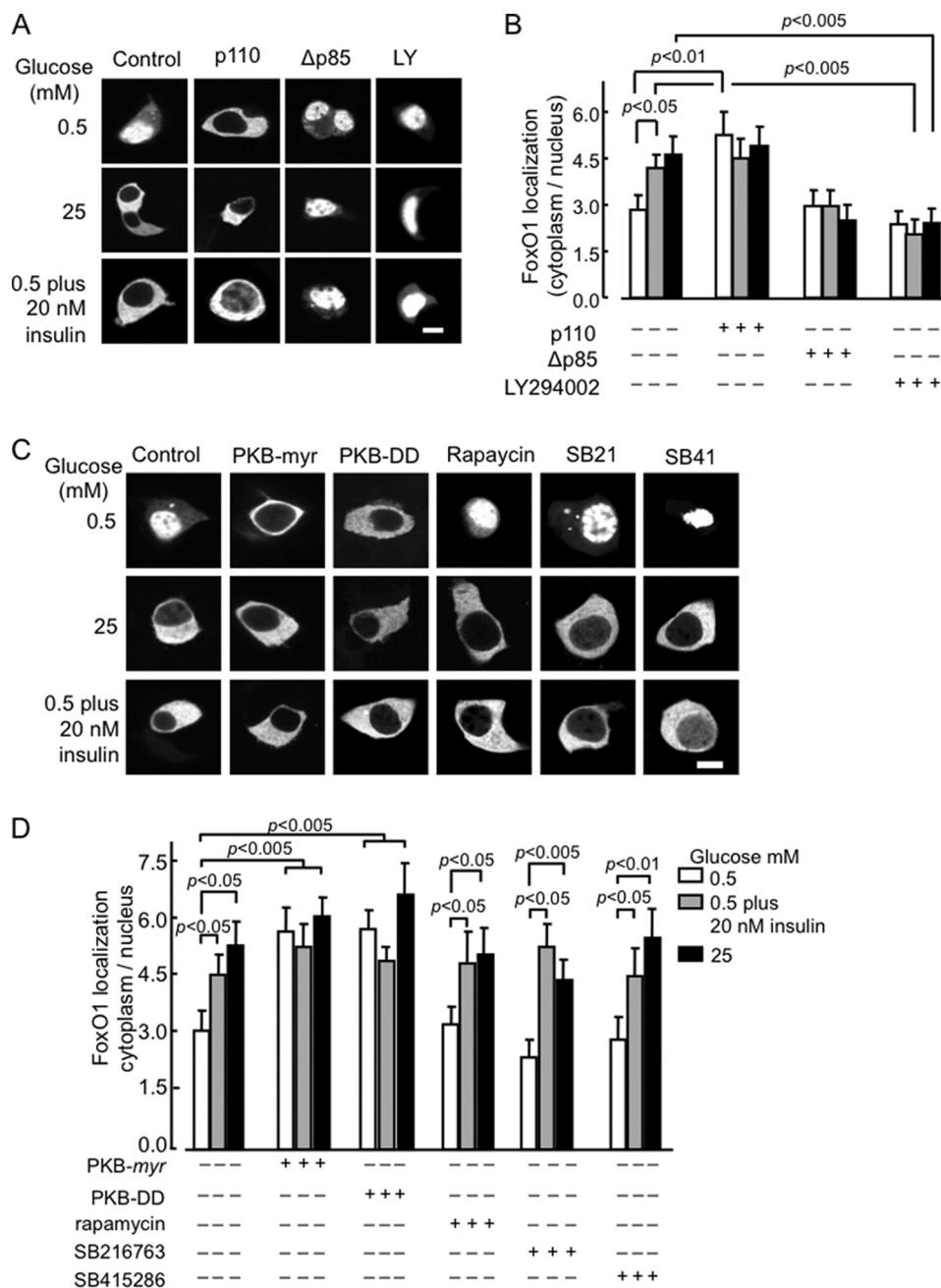


**FIGURE 4. Effects of activation or inhibition of PI 3-Kinase on FoxO1-EGFP localization.** *A*, MIN6 cells, after 24 h of transient transfection with pFoxO1-EGFP (1.0  $\mu$ g), and either empty vector (pcDNA3; Con) or plasmids encoding p100.CAAX or  $\Delta$ p85 (1.0  $\mu$ g) were incubated with further additions (as shown, LY294002, 50  $\mu$ M) for 1 h in KRB medium. *B*, quantitation of the ratio (mean  $\pm$  S.E.,  $n = 20$ –30 cells from  $\geq 3$  separate experiments) as shown in *A*. *C*, effects of glucose and insulin on FoxO1-EGFP localization are mimicked by an active form of protein kinase B but do not require p70 S6 kinase or glycogen synthase kinase-3 (GSK3). Cells were transfected with pFoxO1-EGFP plus either empty vector (pcDNA3; Con), PKB-DD or PKB-myr. After 16 h of incubation in DMEM containing 3 mM glucose, the medium was replaced with medium containing the specified concentrations of glucose, insulin, and GSK3 inhibitors, SB216763 and SB415286 (SB21, SB41, 3  $\mu$ M and 30  $\mu$ M, respectively), rapamycin, 30 nM. *D*, quantitation of ratio (mean  $\pm$  S.E.,  $n = 20$ –40 cells, obtained from  $\geq 3$  independent experiments for each condition). Scale bar, 5  $\mu$ m.

amplification of the previously-known FoxO1 binding regions on the *MafA* and *NeuroD* promoters (supplemental Fig. S3) (37) using the same experimental DNA samples. This observation qualified regions 1 and 2 as physiological FoxO1 binding sites imparting differential regulation of *Ins2* gene expression at low and high concentrations of glucose.

*An Inhibitory Effect of FoxO1, Independent of Pdx1, Is Evident on Ins2 Promoter Activity in a Heterologous System*—We sought next to determine what contribution a direct interaction

of FoxO1 at the *Ins2* promoter may play in the regulation of this gene, independently of a predicted action of FoxO1 to suppress *Pdx1* gene expression. We therefore cloned a 915-bp region spanning (–907 to +8 bp) of the mouse *Ins2* promoter and generated a promoter-reporter construct for luciferase activity assays in MIN6  $\beta$  cells. While the constitutively-active variant of FoxO1 strongly suppressed *Ins2* promoter activity (Fig. 7A), this may conceivably have resulted largely from inhibition of PDX1 expression as reported earlier (20). However, because

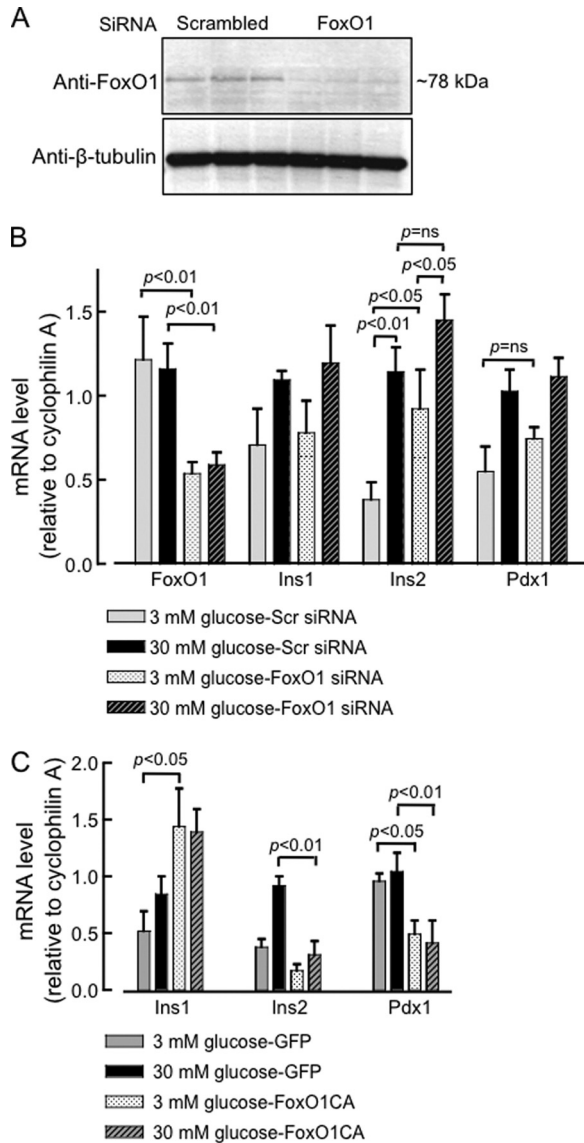


**FIGURE 5. Changes in FoxO1 level modify mouse *Ins2* gene expression.** *A*, Western blot showing protein extracted from MIN6 cells transfected with the indicated siRNA. MIN6 cells were transfected with Smart Pool or scrambled siRNA (20 nM) for 48 h before protein analysis. *B*, real-time qRT-PCR analysis of the indicated genes after siRNA-mediated silencing of FoxO1 studied at 3 and 30 mM glucose concentrations. MIN6 cells were transfected with indicated siRNA as mentioned above. Subsequently, cells were cultured in 3 mM glucose for overnight prior to incubation in 3 or 30 mM glucose for 6–8 h and RNA was extracted for real-time RT-PCR analysis. *C*, MIN6 cells overexpressing a constitutively active (nuclear) FoxO1-CA-EGFP were analyzed by real-time RT-PCR of the indicated genes, as in *B*. Cells were transfected with FoxO1-CA virus (20–25 MOI) for 12 h and subsequently cultured overnight (16 h) in 3 mM glucose prior to incubation in 3 or 30 mM glucose for 6–8 h and RNA was extracted for analysis (see “Experimental Procedures”). Bars (*B*, *C*) show mean  $\pm$  S.E.,  $n \geq 9$  from 4–5 independent experiments of the ddC<sub>T</sub> values (compared with control samples in 30 mM glucose for each gene).

simultaneous overexpression of PDX1 failed to rescue the promoter activity (Fig. 7A), although both FoxO1-EGFP and PDX1 immunoreactively localized in the nucleus (Fig. 7B), the direct inhibitory role of FoxO1 on mouse *Ins2* promoter was clearly evident. In addition, silencing of FoxO1 de-repressed the *Ins2* promoter and yielded a significantly robust activity at each glucose concentration examined (Fig. 7C). Furthermore, when a 290 bp fragment (–907 to –617 bp) from the distal end

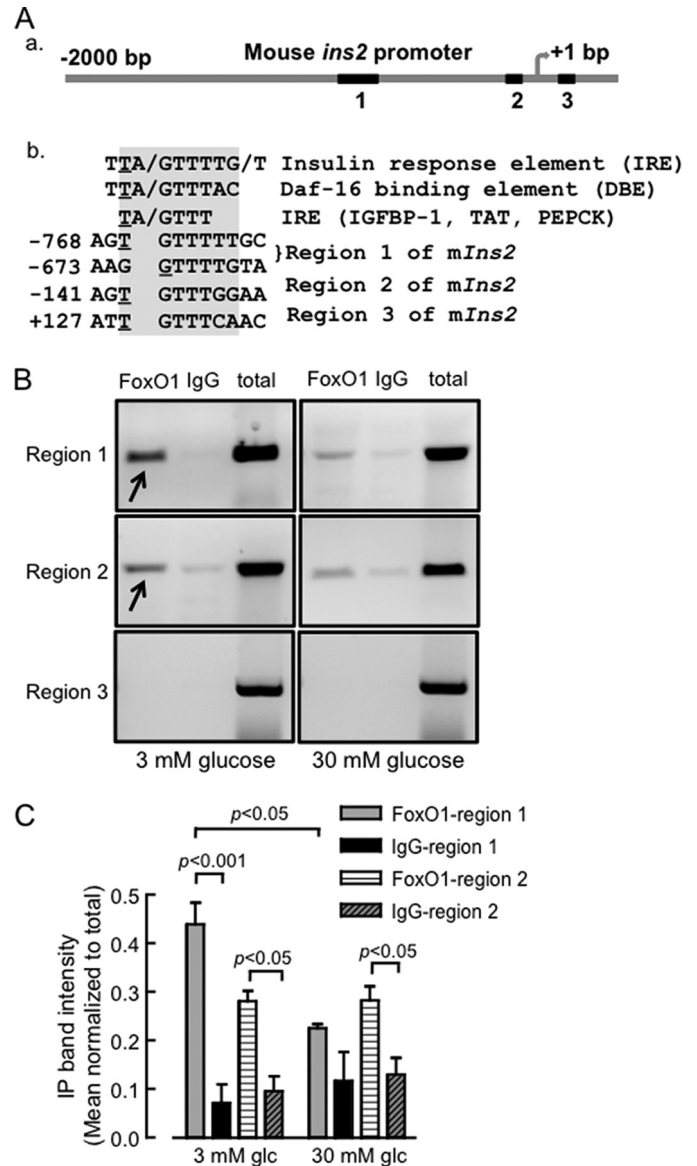


**FIGURE 6. A putative FoxO1 binding site detected in a distal region of mouse *Ins2* promoter.** *A*, comparison of the putative FoxO1 binding elements identified in the mouse *Ins2* promoter (*a*) to the consensus sequences, IRE and DBE (insulin response element, Daf-16 binding element) present in FoxO1-regulated genes. Relative position of the elements corresponds to the underlined nucleotide in the element, with respect to the transcription start site (*b*). *B*, chromatin immunoprecipitation (ChIP) of cross-linked DNA from lysed MIN6 cells using anti-FoxO1 antibody or immunoglobulin (IgG) and subsequent PCR amplification of short (~200 bp) fragments around the putative FoxO1 binding regions. MIN6 cells (70% confluent) were cultured overnight in 3 mM glucose before incubating in 3 or 30 mM glucose for 6 h and subsequently formalin fixed for 15 min. ChIP experiments were done as described under “Experimental Procedures.” The agarose gel image is representative of  $\geq 4$  independent ChIP experiments. *C*, quantification of PCR products, as in *B*, normalized to the matched total, for regions 1 and 2. Bar represents mean  $\pm$  S.E.,  $n = 3$ .

of the *Ins2* promoter, including the putative FoxO1 binding site (region 1) was deleted FoxO1-CA overexpression was no longer able to inhibit the activity of the shorter promoter (Fig. 7D). Finally, the same 290 bp inhibitory region cloned upstream of a thymidine kinase (TK) promoter and a luciferase reporter conferred significant suppression to the TK promoter activity in MIN6  $\beta$  cells (Fig. 7E). Interestingly, silencing of FoxO1 abol-

## FoxO1 Regulation of $\beta$ Cell Genes

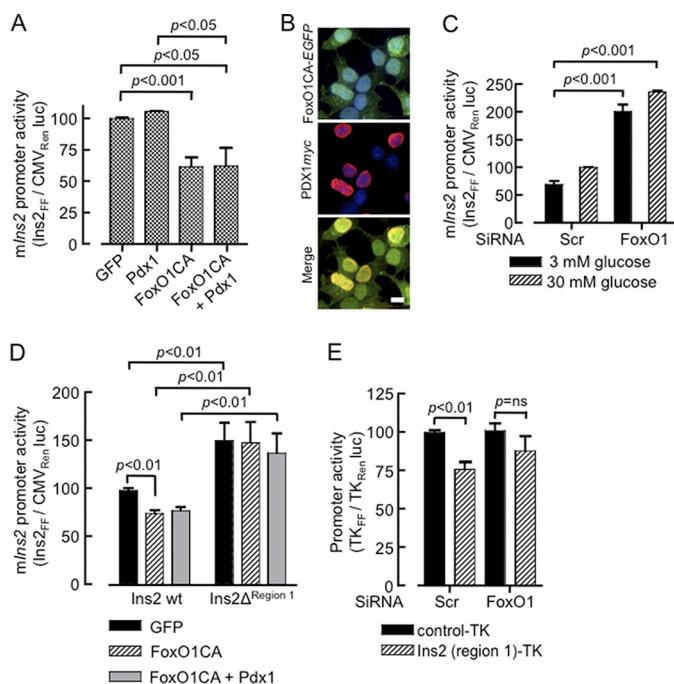


**FIGURE 7. FoxO1 inhibits *Ins2* promoter activity independently of PDX1 analyzed by luciferase assay.** A region of 915 bp of mouse *Ins2* promoter. firefly luciferase reporter construct (pIns2.Luc<sub>Ff</sub>, 450 ng/3.8 cm<sup>2</sup>) was cotransfected with p.CMV.Luc<sub>Ren</sub> (1 ng/3.8 cm<sup>2</sup>) in MIN6 cells and luciferase activity in the lysate was measured as described under "Experimental Procedures." **A**, cells after 6 h of transfection were subsequently infected with the adenoviral vectors (20–25 MOI) as indicated and maintained in high (25 mM) glucose for 16–20 h before analysis ( $n = 5$ ). **C**, MIN6 cells were transfected with siRNA for 48 h preceding transfection of the promoter constructs as described in **A**. Following a 12 h of transfection, cells were incubated for 12–14 h in 3 or 30 mM glucose prior to luciferase assay ( $n = 3$ ). **D**, a deletion mutant of pIns2.Luc<sub>Ff</sub>, lacking region 1 was constructed and promoter activity was compared with the wild type as described in **A** ( $n = 5$ ). **E**, inhibition of thymidine kinase (TK) promoter activity by the FoxO1-regulated region 1 of the *Ins2* promoter. The 290-bp region deleted in **D**, was subcloned upstream to a TK promoter driving firefly luciferase (Ins-TK<sub>Ff</sub>). MIN6 cells transfected with FoxO1 or scrambled siRNA for 48 h prior to cotransfection with Ins-TK<sub>Ff</sub> (500 ng/3.8 cm<sup>2</sup>) and thymidine kinase driving *Renilla* luciferase (TK<sub>Ren</sub>, 100 ng/3.8 cm<sup>2</sup>). After 12 h of transfection cells were incubated in 3 or 30 mM glucose for 12–16 h and luciferase activity was assayed ( $n = 3$ ). Bars in **A**, **C**, **D**, and **E** show mean  $\pm$  S.E. from duplicate samples from  $\geq 3$  independent experiments and analyzed by two-tailed  $t$  test. **B**, confocal images showing the intracellular localization of co-expressed FoxO1-CA-EGFP and PDX1.c-myc examined by immunocytochemistry and DAPI staining ( $n \geq 20$  cells from three independent experiments). Scale bar, 10  $\mu$ m.

ished the inhibition of the modified, but not the wild-type, TK promoter (Fig. 7E).

## DISCUSSION

The principal aim of the current study was to examine the potential role of FoxO1 in the stimulation by glucose and insulin of *preproinsulin* gene transcription in pancreatic islet  $\beta$  cells. The present data are consistent with a previous report (21) suggesting that the effects of glucose on the subcellular localization of FoxO1 in  $\beta$  cells are mediated largely by secreted insulin. Extending these earlier findings, the inhibitor studies performed here also suggest that whereas activation of the PKB pathway is likely to be critical for the nuclear-cytosolic translocation of FoxO1, p70 S6 kinase and GSK3 are not involved. The latter finding is consistent with a previous report that FoxO1 is not a target of GSK-3 in the stimulation of IGFBP-1 expression by insulin in the liver (38).

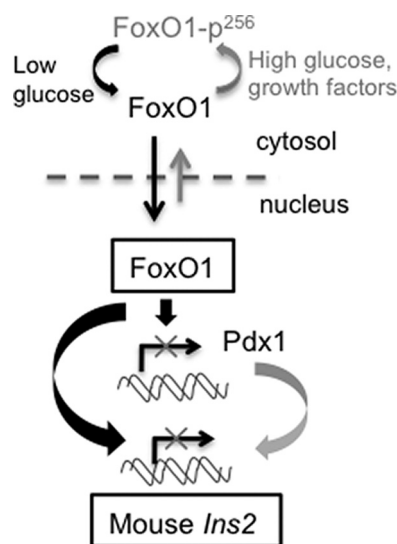


**FIGURE 8. Schematic diagram showing FoxO1 mediated direct regulation of rodent *Ins2* gene expression depending on available nutrient (glucose) and growth factors.**

We and others (4, 32) have previously demonstrated that glucose stimulates the accumulation of mRNAs encoding both the *preproinsulin* and *Pdx1* (32) genes through a mechanism likely to involve the release of insulin. However, the identity of the transcriptional stimulators/repressors which mediate these effects is only partially elucidated. Thus, PDX-1, HNF1 $\alpha$  (39), and FoxA2 (36) have each been identified as regulators of *Pdx1* transcription, and likely to be important in the cell type-specific expression of this factor. We have previously shown that glucose (24, 40), but not insulin (41), also causes the translocation of PDX1 from the cytosol and nuclear periphery into the nucleoplasm. The present results suggest that FoxO1 may play an important role in the regulation by glucose and insulin of both the *Ins2* and the *Pdx1* genes. Thus, overexpressed FoxO1 blocked the effects of either stimulus on each promoter (*Ins2*-Fig. 7A, *Pdx1*, data not shown).

An unexpected and novel finding of the present work was that overexpression of the constitutively active FoxO1 effectively suppressed the induction of the mouse *Ins2*, but not *Ins1* by glucose (Fig. 5C), while activation (de-repression) of *Ins2* expression was observed in FoxO1-silenced cells. Interestingly, the effect of FoxO1-CA, leading to a decrease in *Ins2* mRNA levels, was accompanied by a concomitant increase in *Ins1* mRNA message. These observations in MIN6 cell lines are consistent with findings in an earlier report demonstrating a compensatory rise in *Ins1* mRNA levels in *Ins2*<sup>-/-</sup> mice (42). This finding suggests that the repressive effect of FoxO1-CA on *Ins2* expression is unlikely to be due simply to a decrease in PDX1 levels, as might be predicted from earlier findings (20), because such a mechanism would be expected to inhibit both *Ins1* and *Ins2* expression. Furthermore, the inhibitory action of FoxO1 was resistant to overexpression of exogenous PDX1 to levels capable of stimulating the *Ins2* promoter to essentially the same extent as high glucose (Fig. 7A), under conditions where the presence of both FoxO1 and PDX1 could readily be demonstrated in the nucleus (Fig. 7B).

A model describing the putative role of FoxO1 in the regulation of the rodent *Ins2* gene is provided in Fig. 8. This FoxO1-dependent mechanism for the control of insulin genes seems likely to play a role in an action of glucose, via the stimulated secretion of insulin and then rebinding of the hormone to its receptors on the  $\beta$  cells (8, 43) to activate further insulin gene transcription in an autocrine loop. Providing further evidence for such a mechanism, Hettiarachchi *et al.* (44) demonstrated that short term treatment of MIN6  $\beta$  cells with bafilomycin led to prolonged activation of the insulin receptor, insulin receptor substrate 2 and Akt. Bafilomycin treatment also led to nuclear exclusion of FoxO1 and increased *preproinsulin* gene expression.

A search for consensus binding sites for the DAF-16 homologues FoxO1, FoxO3a, FoxO4 (Formerly FKHR, FKHL1, and AFX1) (45), and IRE (46) in the mouse (and rat) *preproinsulin* promoters resulted in the identification of two regions in the *Ins2* gene that showed glucose-regulated binding to FoxO1, and which conferred sensitivity to suppression by the constitutively active FoxO1. Interestingly, closely similar sequences lie in the regions of the human insulin promoter previously termed GGII (−148CCTTTAC) and GGI (−135TTTAAC) (47), the latter a “mini-enhancer region” now referred to as the A2 box (48). Yet another conserved site was detected in the second intron of the human (+749TGTTTTG) and Chimpanzee *INS* genes. None of these regions was present in mouse or rat *Ins1* genes. It is important to emphasize that the origin and regulation of the *Ins2* and *Ins1* genes in rodents differs: the *Ins1* gene seems likely to be a functional retroposon of *Ins2* emerging later in evolution (49), and unlike *Ins2* the former lacks genetic imprinting and expresses from both alleles (50). “Snapshot” measurements of the precise number of *Ins1* and *Ins2* mRNA molecules expressed in single primary  $\beta$  cells from mouse islets incubated at low (5 mM) and high (20 mM) glucose concentrations also indicated differential expression and inducibility of the two insulin genes previously, *Ins2* mRNA being 3-fold and 2-fold higher than *Ins1* mRNA at low and high glucose, respectively (51).

Notably *Ins2*, but not *Ins1*, appears to be expressed in the hypothalamus and other parts of the brain during development and possibly at later stages (52, 53). Differences in the regulatory regions lying upstream of the two genes, as further detailed in the present study, seem likely to underlie the differing expression patterns of the *Ins1* and *Ins2* genes in rodents.

*Acknowledgments*—We thank Dr. Mark Jepson and Alan Leard of the Bristol MRC Imaging Centre for technical and other support. We thank JDRF for the provision of human islets (JDRF award 31-2008-617 UK Islets for basic research programme) (to S. H and P. J.).

## REFERENCES

- Rutter, G. A., Tavares, J. M., and Palmer, D. G. (2000) *News Physiol. Sci.* **15**, 149–154
- Melloul, D., Marshak, S., and Cerasi, E. (2002) *Diabetologia* **45**, 309–326
- Kulkarni, R. N., Brüning, J. C., Winnay, J. N., Postic, C., Magnuson, M. A., and Kahn, C. R. (1999) *Cell* **96**, 329–339
- Leibiger, B., Moede, T., Schwarz, T., Brown, G. R., Köhler, M., Leibiger, I. B., and Berggren, P. O. (1998) *Proc. Natl. Acad. Sci. U.S.A.* **95**, 9307–9312
- Rutter, G. A. (1999) *Curr. Biol.* **9**, R443–R445
- da Silva, Xavier, G., Varadi, A., Ainscow, E. K., and Rutter, G. A. (2000) *J. Biol. Chem.* **275**, 36269–36277
- Andreolas, C., da Silva, Xavier, G., Diraison, F., Zhao, C., Varadi, A., Lopez-Casillas, F., Ferré, P., Foufelle, F., and Rutter, G. A. (2002) *Diabetes* **51**, 2536–2545
- da Silva, Xavier, G., Qian, Q., Cullen, P. J., and Rutter, G. A. (2004) *Biochem. J.* **377**, 149–158
- Bouche, C., Lopez, X., Fleischman, A., Cypess, A. M., O’Shea, S., Stefanovski, D., Bergman, R. N., Rogatsky, E., Stein, D. T., Kahn, C. R., Kulkarni, R. N., and Goldfine, A. B. (2010) *Proc. Natl. Acad. Sci. U.S.A.* **107**, 4770–4775
- Lantz, K. A., and Kaestner, K. H. (2005) *Clin. Sci.* **108**, 195–204
- Nakae, J., Biggs, W. H., 3rd, Kitamura, T., Cavenee, W. K., Wright, C. V., Arden, K. C., and Accili, D. (2002) *Nat. Genet.* **32**, 245–253
- Cahill, C. M., Tzivion, G., Nasrin, N., Ogg, S., Dore, J., Ruvkun, G., and Alexander-Bridges, M. (2001) *J. Biol. Chem.* **276**, 13402–13410
- Trümper, A., Trümper, K., Trusheim, H., Arnold, R., Göke, B., and Hörsch, D. (2001) *Mol. Endocrinol.* **15**, 1559–1570
- Rena, G., Guo, S., Cichy, S. C., Unterman, T. G., and Cohen, P. (1999) *J. Biol. Chem.* **274**, 17179–17183
- Matsuzaki, H., Daitoku, H., Hatta, M., Tanaka, K., and Fukamizu, A. (2003) *Proc. Natl. Acad. Sci. U.S.A.* **100**, 11285–11290
- Brunet, A., Bonni, A., Zigmond, M. J., Lin, M. Z., Juo, P., Hu, L. S., Anderson, M. J., Arden, K. C., Blenis, J., and Greenberg, M. E. (1999) *Cell* **96**, 857–868
- McKinnon, C. M., Ravier, M. A., and Rutter, G. A. (2006) *J. Biol. Chem.* **281**, 39358–39369
- Xuan, S., Kitamura, T., Nakae, J., Politi, K., Kido, Y., Fisher, P. E., Morrioni, M., Cinti, S., White, M. F., Herrera, P. L., Accili, D., and Efstratiadis, A. (2002) *J. Clin. Invest.* **110**, 1011–1019
- Buteau, J., Shlien, A., Foisy, S., and Accili, D. (2007) *J. Biol. Chem.* **282**, 287–293
- Kitamura, T., Nakae, J., Kitamura, Y., Kido, Y., Biggs, W. H., 3rd, Wright, C. V., White, M. F., Arden, K. C., and Accili, D. (2002) *J. Clin. Invest.* **110**, 1839–1847
- Martinez, S. C., Cras-Méneur, C., Bernal-Mizrachi, E., and Permutt, M. A. (2006) *Diabetes* **55**, 1581–1591
- Ainscow, E. K., and Rutter, G. A. (2001) *Biochem. J.* **353**, 175–180
- Kennedy, H. J., Viollet, B., Rafiq, I., Kahn, A., and Rutter, G. A. (1997) *J. Biol. Chem.* **272**, 20636–20640
- Rafiq, I., da Silva, Xavier, G., Hooper, S., and Rutter, G. A. (2000) *J. Biol. Chem.* **275**, 15977–15984
- Dhand, R., Hara, K., Hiles, I., Bax, B., Gout, I., Panayotou, G., Fry, M. J., Yonezawa, K., Kasuga, M., and Waterfield, M. D. (1994) *EMBO J.* **13**, 511–521
- Miyazaki, J., Araki, K., Yamato, E., Ikegami, H., Asano, T., Shibasaki, Y., Oka, Y., and Yamamura, K. (1990) *Endocrinology* **127**, 126–132
- Cross, S. E., Hughes, S. J., Partridge, C. J., Clark, A., Gray, D. W., and Johnson, P. R. (2008) *Transplantation* **86**, 907–911
- Ravier, M. A., and Rutter, G. A. (2005) *Diabetes* **54**, 1789–1797
- Meur, G., Simon, A., Harun, N., Virally, M., Dechaume, A., Bonnefond, A., Fetita, S., Tarasov, A. I., Guillausseau, P. J., Boesgaard, T. W., Pedersen, O., Hansen, T., Polak, M., Gautier, J. F., Froguel, P., Rutter, G. A., and Vaxillaire, M. (2010) *Diabetes* **59**, 653–661
- Noordeen, N. A., Khera, T. K., Sun, G., Longbottom, E. R., Pullen, T. J., da Silva, Xavier, G., Rutter, G. A., and Leclerc, I. (2010) *Diabetes* **59**, 153–160
- Elayat, A. A., el-Naggar, M. M., and Tahir, M. (1995) *J. Anat.* **186**, 629–637
- da Silva, Xavier, G., Leclerc, I., Varadi, A., Tsuboi, T., Moule, S. K., and Rutter, G. A. (2003) *Biochem. J.* **371**, 761–774
- Briaud, I., Lingohr, M. K., Dickson, L. M., Wrede, C. E., and Rhodes, C. J. (2003) *Diabetes* **52**, 974–983
- Lingohr, M. K., Dickson, L. M., McCuaig, J. F., Hugl, S. R., Twardzik, D. R., and Rhodes, C. J. (2002) *Diabetes* **51**, 966–976
- Coghlan, M. P., Culbert, A. A., Cross, D. A., Corcoran, S. L., Yates, J. W., Pearce, N. J., Rausch, O. L., Murphy, G. J., Carter, P. S., Roxbee, C. L., Mills, D., Brown, M. J., Haigh, D., Ward, R. W., Smith, D. G., Murray, K. J., Reith, A. D., and Holder, J. C. (2000) *Chem. Biol.* **7**, 793–803
- Lee, C. S., Sund, N. J., Vatamaniuk, M. Z., Matschinsky, F. M., Stoffers,

## FoxO1 Regulation of $\beta$ Cell Genes

- D. A., and Kaestner, K. H. (2002) *Diabetes* **51**, 2546–2551
37. Kitamura, Y. I., Kitamura, T., Kruse, J. P., Raum, J. C., Stein, R., Gu, W., and Accili, D. (2005) *Cell Metab.* **2**, 153–163
38. Finlay, D., Patel, S., Dickson, L. M., Shpiro, N., Marquez, R., Rhodes, C. J., and Sutherland, C. (2004) *BMC. Mol. Biol.* **5**, 15
39. Shih, D. Q., Heimesaat, M., Kuwajima, S., Stein, R., Wright, C. V., and Stoffel, M. (2002) *Proc. Natl. Acad. Sci. U.S.A.* **99**, 3818–3823
40. Rafiq, I., Kennedy, H. J., and Rutter, G. A. (1998) *J. Biol. Chem.* **273**, 23241–23247
41. Guillemain, G., da Silva, Xavier, G., Rafiq, I., Leturque, A., and Rutter, G. A. (2004) *Biochem. J.* **378**, 219–227
42. Leroux, L., Desbois, P., Lamotte, L., Duvillié, B., Cordonnier, N., Jackerott, M., Jami, J., Bucchini, D., and Joshi, R. L. (2001) *Diabetes*. **50**, S150–S153
43. Leibiger, I. B., Leibiger, B., Moede, T., and Berggren, P. O. (1998) *Mol. Cell* **1**, 933–938
44. Hettiarachchi, K. D., Zimmet, P. Z., and Myers, M. A. (2006) *Cell Biol. Toxicol.* **22**, 169–181
45. Furuyama, T., Nakazawa, T., Nakano, I., and Mori, N. (2000) *Biochem. J.* **349**, 629–634
46. Durham, S. K., Suwanichkul, A., Scheimann, A. O., Yee, D., Jackson, J. G., Barr, F. G., and Powell, D. R. (1999) *Endocrinology* **140**, 3140–3146
47. Boam, D. S., Clark, A. R., and Docherty, K. (1990) *J. Biol. Chem.* **265**, 8285–8296
48. German, M., Ashcroft, S., Docherty, K., Edlund, H., Edlund, T., Goodison, S., Imura, H., Kennedy, G., Madsen, O., Melloul, D., Moss, L., Olson, K., Permutt, M. A., Philippe, J., Robertson, R. P., Rutter, W. J., Serup, P., Stein, R., and Steiner, D. (1995) *Diabetes* **44**, 1002–1004
49. Soares, M. B., Schon, E., Henderson, A., Karathanasis, S. K., Cate, R., Zeitlin, S., Chirgwin, J., and Efstratiadis, A. (1985) *Mol. Cell. Biol.* **5**, 2090–2103
50. Deltour, L., Vandamme, J., Jouvenot, Y., Duvillié, B., Kelemen, K., Schaeferly, P., Jami, J., and Paldi, A. (2004) *Gene Expr. Patterns* **5**, 297–300
51. Bengtsson, M., Ståhlberg, A., Rorsman, P., and Kubista, M. (2005) *Genome Res.* **15**, 1388–1392
52. Gannon, M., Shiota, C., Postic, C., Wright, C. V., and Magnuson, M. (2000) *Genesis* **26**, 139–142
53. Wicksteed, B., Brissova, M., Yan, W., Opland, D. M., Plank, J. L., Reinert, R. B., Dickson, L. M., Tamarina, N. A., Philipson, L. H., Shostak, A., Bernal-Mizrachi, E., Elghazi, L., Roe, M. W., Labosky, P. A., Myers, M. M., Jr., Gannon, M., Powers, A. C., and Dempsey, P. J. (2010) *Diabetes* **59**, 3090–3098